Available online at www.sciencedirect.com

ScienceDirect

Energy Procedia 114 (2017) 2856 – 2870

Energy Procedia

13th International Conference on Greenhouse Gas Control Technologies, GHGT-13, 14-18 November 2016, Lausanne, Switzerland

An improved history-match for layer spreading within the Sleipner plume including thermal propagation effects

Gareth.A. Williams[a]* R. Andrew. Chadwick[b]

[a]*British Geological Survey, The Lyell Centre, Research Avenue South, Edinburgh, EH14 4AP, UK*
[b]*British Geological Survey, Environmental Science Centre, Nicker Hill, Keyworth, Nottingham , NG12 5GG*

Abstract

The Sleipner CO_2 storage operation has been injecting CO_2 since 1996, and the growth of the plume has been intensively monitored using time-lapse seismic techniques. Detailed history-matching of the topmost CO_2 layer has proven challenging. This paper summarizes results from a series of flow simulations examining two key parameters affecting CO_2 mobility: permeability heterogeneity and fluid temperatures within the plume. The best match to the observed distribution of CO_2 was achieved by including high permeability channels in the reservoir flow model, as observed on seismic data. Thermal models suggests that CO_2 enters the top sand layer 7 ºC warmer than the ambient reservoir. The resulting reduction in the density and viscosity of CO_2 does not significantly improve the fit between seismic and simulation.

Peer-review under responsibility of the organizing committee of GHGT-13.

Keywords: Sleipner; numerical flow simulation; CO_2 plume; layer spreading; history match; thermal; chanelling; permeability.

1. Introduction

The Sleipner CO_2 storage operation has been injecting around 0.8-1.0 million tons of CO_2 every year since 1996, making it the world's longest running CO_2 sequestration project. The growth of the CO_2 plume has been intensively monitored using 4D time-lapse seismic techniques, with data acquired in 1994 (baseline), 1999, 2001, 2004, 2006,

* Corresponding author. Tel +44(0)131-667-265; fax: +44 (0)115 -936- 3200.
E-mail address: gwil@bgs.ac.uk

Peer-review under responsibility of the organizing committee of GHGT-13.
doi:10.1016/j.egypro.2017.03.1406

2008, 2010 and more recently in 2013. These surveys have successfully imaged the growing plume, which has spread beneath the low permeability shale caprock in a preferentially north-south direction (Fig. 1).

Statoil released the Sleipner modelling benchmark dataset in 2011 [1], comprising a numerical mesh and related input data to allow modelers to test different codes and approaches to history matching the observed plume growth. The benchmark model represents the top sand layer within the reservoir, where the distribution of CO_2 is clearly imaged by seismic data, providing important constraints on the reservoir model. A number of workers have attempted to history-match the growth of this topmost CO_2 layer, with varying degrees of success [1, 2, 3, 4, 5, 6]. In general, the simulations fail to predict the speed of the rapid northward migration of CO_2 along a prominent linear ridge beneath the reservoir caprock (Fig. 1). Previous modelling has investigated the effects of small uncertainties in topseal topography, permeability anisotropy, gas composition and reservoir temperature [2, 3, 4]. Alternative (non-Darcy flow) modelling approaches have also been advocated, including vertical equilibrium solutions and invasion percolation models [5, 6]. These modifications have had varying degrees of success in replicating the observed layer growth rates.

Zhu et al. [4] performed an extensive sensitivity analysis of various parameters affecting CO_2 mobility, with the aim of matching the seismic evidence. They showed that spreading rates of CO_2 were sensitive to temperature and the presence of impurities. Matching the observed CO_2 – water contact (CWC) required high reservoir temperatures (>35 ºC) and / or high methane content (>4%) in order to reduce the viscosity of the CO_2 sufficiently to achieve the mobility required to match the observed spreading rates. Invoking such a high reservoir temperature is problematic. The temperature in the top sand-wedge is thought to be around 30 ºC +/- 0.5 ºC, based on robust measurements from the nearby water production operation at the Volve field. [7]

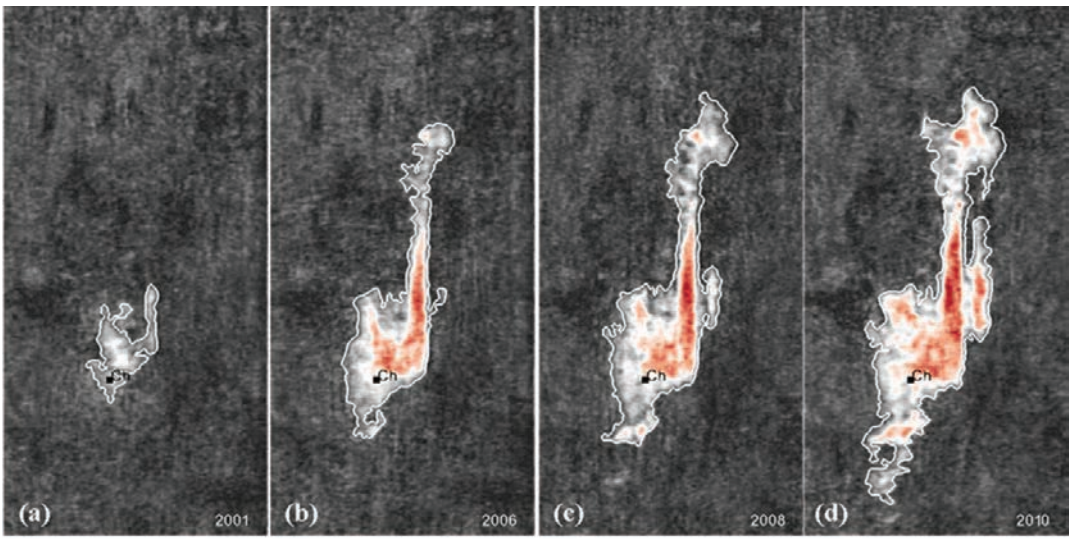

Fig. 1. Extent of the topmost CO_2 layer in the Sleipner plume as imaged on 3D time-lapse seismic data in 2001, 2006, 2008 and 2010. The thin layer of CO_2 has ponded beneath the caprock, which acts as a barrier to upward advection. The seismically resolvable plume limits are shown by the white polygon: these limits are used for comparison with simulations in later figures. The position of the chimney through which the CO_2 enters the top sand layer is marked with a black square (Ch).

This paper investigates the combined effects of two key controls on CO_2 mobility: intrinsic permeability and temperature distribution within the mobile CO_2 phase (as distinct from the background reservoir temperature).

Permeability heterogeneity is a key factor controlling the flow of CO_2 in sandstone reservoirs. Previous attempts to history-match the rapid growth of the topmost layer at Sleipner [3] have considered orthogonal permeability anisotropy, but not the explicit effects of geological features such as channeling. In fact high resolution seismic data acquired in 2010 has shown that the top sand-wedge comprises a series of channels running from north-south across the survey area (Fig. 2).

The temperature of the CO_2 at the injection perforations (~1058 m.b.s.l) is estimated at around 48 ºC (or slightly higher depending on pressure) due to adiabatic compression within the injection tubing [7]. This is around 13 ºC warmer than the ambient reservoir temperature at the injection point and would create a thermal anomaly, potentially propagating to the reservoir top reducing CO_2 density and viscosity and increasing mobility.

Nomenclature

CWC	CO_2 - water contact
m.b.s.l	metres below mean sea level
S_g	CO_2 saturation [-]
k_{rg}	CO_2 relative permeability [-]
S_w	Brine saturation [-]
k_{rw}	Brine relative permeability [-]
P_{CG}	CO_2 capillary pressure [bar]
ms	milli-seconds two-way travel time

2. Flow properties of the Utsira Sand

2.1. Porosity and permeability

Laboratory porosity and permeability measurements of the Utsira Sand were made by the Saline Aquifer CO_2 Storage Project (SACS) [8, 9]. The core was taken from Norwegian well 15/9-A23 between 905-910 m.b.s.l: the well head is located around 2.5 km south west of the injection point. The average porosity was found to be 0.38 and the permeability 2.9 Darcy. However well pumping tests in the Utsira Sand in the Oseberg fields (located around 250 km NE of Sleipner) give a bulk reservoir permeability range between 1.1 and 8.1 Darcy [9]. Similar tests in the Grane field, which lies around 100 km to the NE of Sleipner, gave a bulk reservoir permeability for the Utsira Sand of around 6 Darcy [9].

2.2. Reservoir compartmentalization

Well and seismic data show the Utsira Sand to be divided vertically into a series of sand units separated by thin mudstones, the CO_2 forming seismically distinct layers trapped beneath these semi-permeable baffles (Fig. 2). Flow simulation studies of the Sleipner site have traditionally focused on matching the growth of the topmost CO_2 layer in the plume, which is trapped in a sand body directly beneath the caprock. A recent study by the Norweigian Petroleum Directorate [10] found that this sand layer is a separate stratigraphic unit some 1 Ma younger than the Utsira Sand itself and is hereafter referred to as the top sand-wedge (Fig. 2).

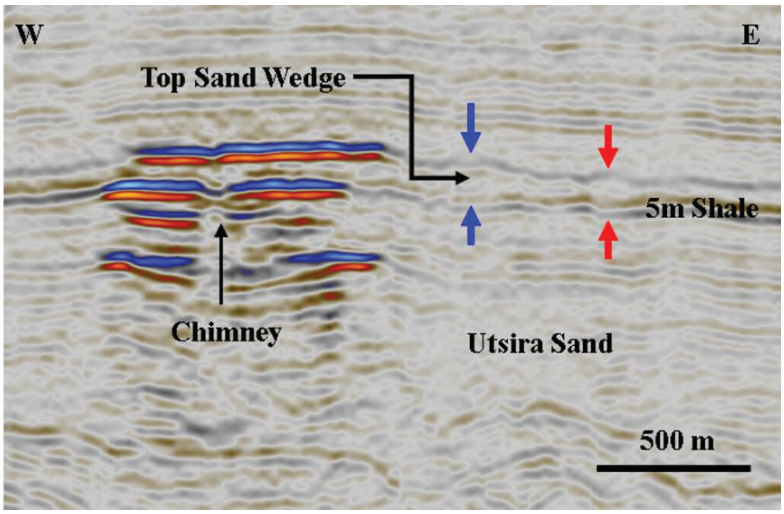

Fig. 2. High resolution seismic image showing the top sand-wedge together with CO_2 layers in the Utsira Sand. The CO_2 has ponded beneath thin mudstone layers which act as barriers to upward advection. A 5-7 m thick mudstone separates the upper sand-wedge from the main Utsira Sand beneath and this has been breached through a distinct chimney feature. The top sand-wedge appears to be extensively channeled; two examples of localised channeling are highlighted by blue and red arrows.

The position of the core used to measure formation porosity and permeability (Fig. 3) lies below the top sand-wedge, on the flank of a zone of disrupted reflections interpreted as a mud diapir intruded into the Utsira Sand from below [8]. The gamma-ray log (Fig. 4) suggests that the reservoir in the vicinity of the core has a higher mud content than the top sand-wedge in the well, which has a markedly cleaner gamma ray signature. Consequently it is reasonable to assume that the measured permeability of ~3 Darcy is not representative of the top sand-wedge. For our flow simulations we use a lower bound permeability of 3 Darcy and an upper bound of 8 Darcy, the latter value being consistent with the Oseberg and Grane field pumping tests [9].

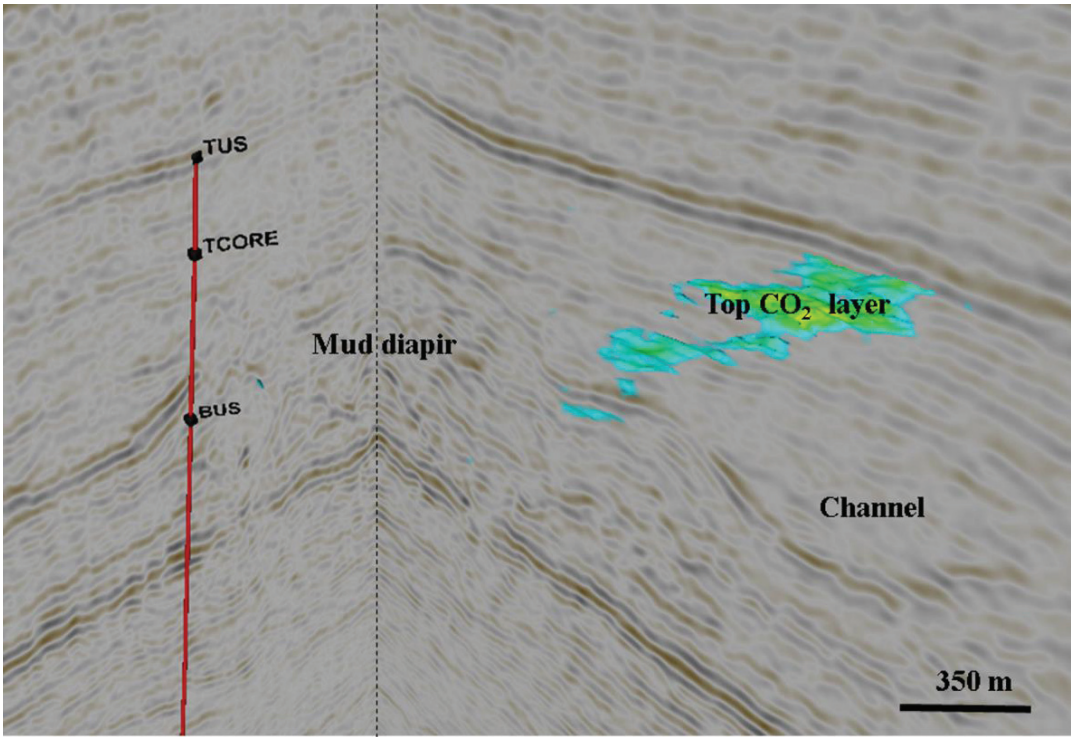

Fig. 3. Position of the core in Norwegian well 15/9-A23 between 905 and 910 m.b.s.l. The cored interval lies on the flank of a mud diapir. The topmost CO_2 layer lies in a channel of sand unaffected by mud diapirism.

2.3. Channeling

The seismic data show clear evidence of channeling in the Utsira Sand. Isochore maps for both the whole reservoir interval (Fig. 5a) and the top sand-wedge (Fig. 5b) show channels preferentially oriented north-south with positions controlled by the deeper-seated mud diapirs. Lithological and bio-stratigraphical analysis of the Utsira Sand suggest that it was deposited in a marine high energy environment, possibly by gravity flow in turbidity currents [8]. This is consistent with the observed channeling at Sleipner and suggests that there might be significant fabric anisotropy in the main channels, with a preferential north-south flow direction. It is further notable that the top sand-wedge in the vicinity of the plume occupies a depositional channel, whereas the top sand-wedge in the cored well does not. This would be consistent with the top sand-wedge at the CO_2 plume being even cleaner sand than in the core well. The topmost CO_2 layer follows ridges in the topseal which directly overlie the channels in the top sand-wedge, the latter being typically more than around 20 metres thick.

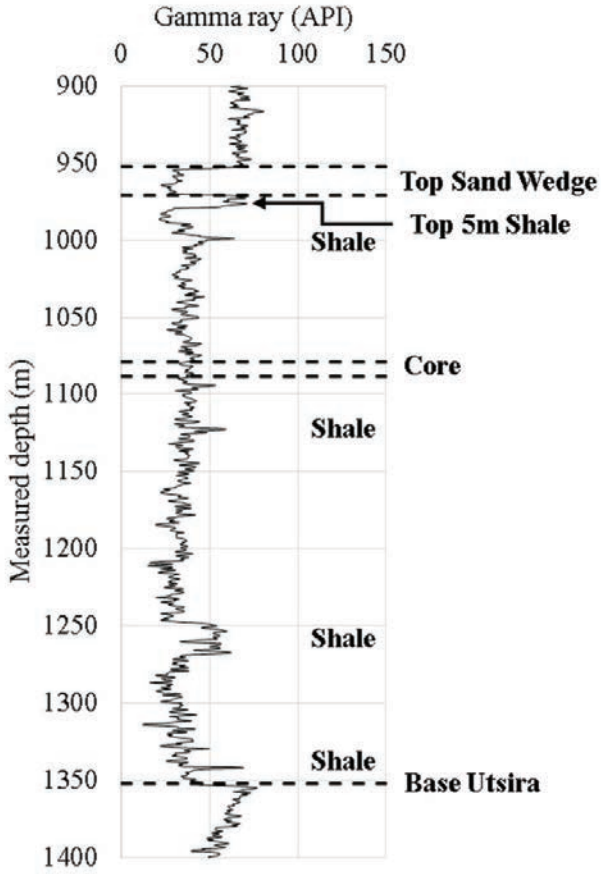

Fig. 4 Gamma ray log through the Utsira Sand in Norwegian well 15/9-A23. The cored section with measurements of porosity and permeability was located between 1080 and 1088 m drilled depth, 905 and 910 m.b.s.l. The top sand-wedge can be readily identified on the gamma-ray log, separated from the rest of the reservoir by a thick (~5 m) low permeability mudstone.

2.4. Relative permeability and capillary pressure

Relative permeability curves for the CO_2 and brine are based on end-point saturations from the Sleipner Benchmark model [1]. These are shown (Fig. 6) together with upscaled relative permeability curves used in the simulators. Brine saturation capillary pressure data was published as part of the SACS report [9], and these were fitted using a Van Genuchten formulation with a capillary entry pressure of 1300 Pa and an exponent of 0.6 (Fig. 6).

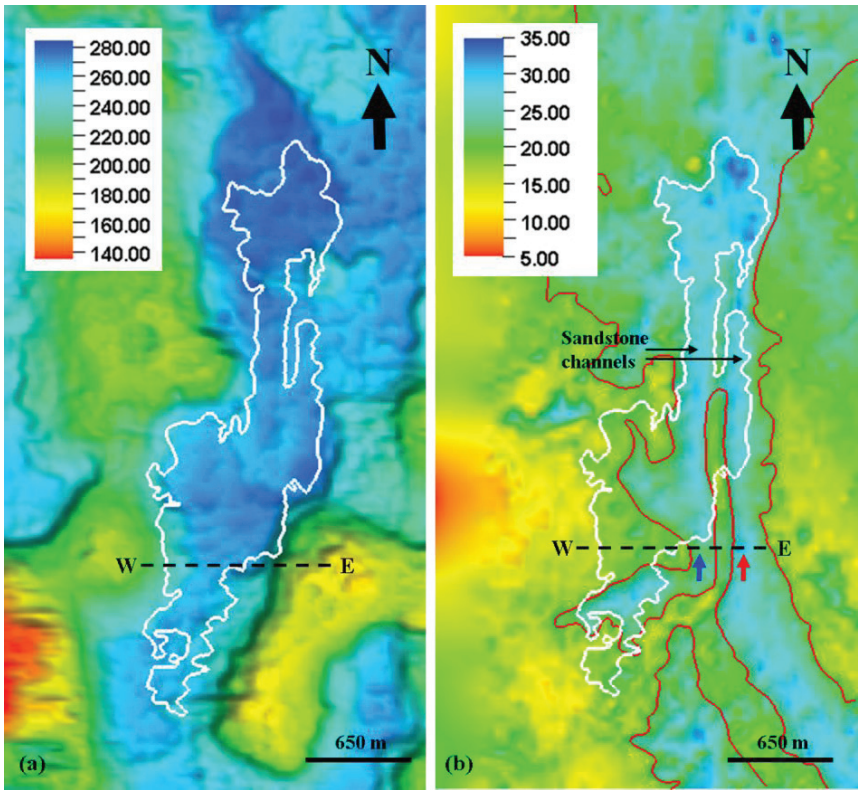

Fig. 5. Shaded isochore maps (ms) of the whole Utsira Sand (a) and top sand-wedge (b) from seismic mapping. Cold colours denote thicker reservoir (channels). Warm colours highlight thinning in the reservoir above mud diapirs. The red polygon in (b) outlines the 20 ms isochore. The white polygon delineates the margins of the topmost CO_2 layer in 2010. The dotted line shows the location of the seismic section (Fig. 2). The blue and red arrows show individual channels in the top sand-wedge (Fig. 2).

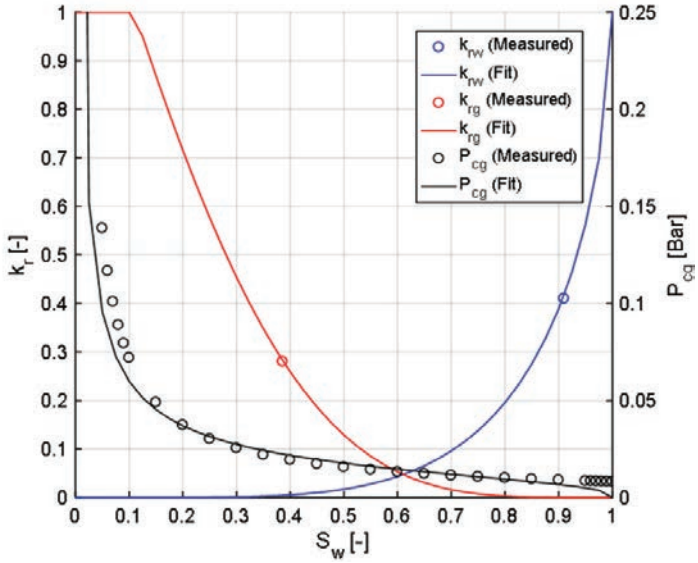

Fig. 6. Relative permeability and brine saturation capillary pressure data used in the simulations. Relative permeability endpoints S_g 0.61, k_{rg} 0.28; S_w 0.91, k_{rw} 0.41 were measured in the laboratory [1].

3. Temperature structure and transport properties of the CO_2 plume

Alnes et al.[7] published expressions for the reservoir pressure and temperature in the vicinity of Sleipner as a function of depth, based on robust measurements from the water production well 15/9-F-7 at the Volve field, 10 km north of the Sleipner injection well. Based on these relationships, the temperature and pressure range in the top sand-wedge is calculated at 28.4 - 30.7 ºC and 82 - 89 bar respectively. The mean whole reservoir temperature is 30 ºC +/- 0.5 ºC and the reservoir temperature at the injection point is around 35 ºC and the pressure 105 bars.

CO_2 is close to the critical point at these conditions, and a phase change from liquid to gas would result in a significant drop in density and viscosity and increased mobility. Consequently it is important to establish the temperature of the CO_2 within the plume itself. Alnes et al. calculated that the CO_2 is injected at a temperature of 48 ºC, based on solving flow equations along the well from the wellhead (P = 64 bar, T = 25 ºC) to the injection point (P = 105 bar). This is significantly warmer than the ambient reservoir.

A reservoir model was run in the PFLOTRAN reservoir simulator [11] in order to model detailed temperature structure within the plume (Fig. 7). The model incorporates a 2D radial axisymmetric mesh, with 80 cells in the horizontal direction increasing in width logarithmically with distance from the injection cell (Fig. 7a). The simulation grid is divided vertically into 170 cells with variable dimensions, chosen to give detailed resolution around the injection point and the thin mudstone layers in the reservoir. The top of the reservoir is positioned at a depth of 797 m below sea level; the topmost sand unit being capped by 50 m of very low permeability caprock. No-flow boundary conditions were placed at the top, base and perimeter of the model, although the grid extends to a radial distance of $2.5x10^5$ m, effectively behaving as an “open aquifer” over the injection timescale. A variable injection rate with a mean value of 27 kgs^{-1} was used, based on the actual values measured at the injection wellhead (Ola Eiken, Statoil, personal communication). The upper sand layers labelled (Fig. 7a) were assigned a permeability of 3 Darcy and the lower sand layers a permeability of 1 Darcy, adjusted to match the relative extents of each CO_2 layer to the observed seismic data. The thin intra-reservoir mudstones were assigned a permeability of 0.0065 Darcy, chosen by iteration to match the arrival time of CO_2 at the top of the reservoir in 1999 observed on seismic data. A thermal conductivity of 3 W/m.K was used for reservoir sand and 1.5 W/m.K for mudstone [15, 16].

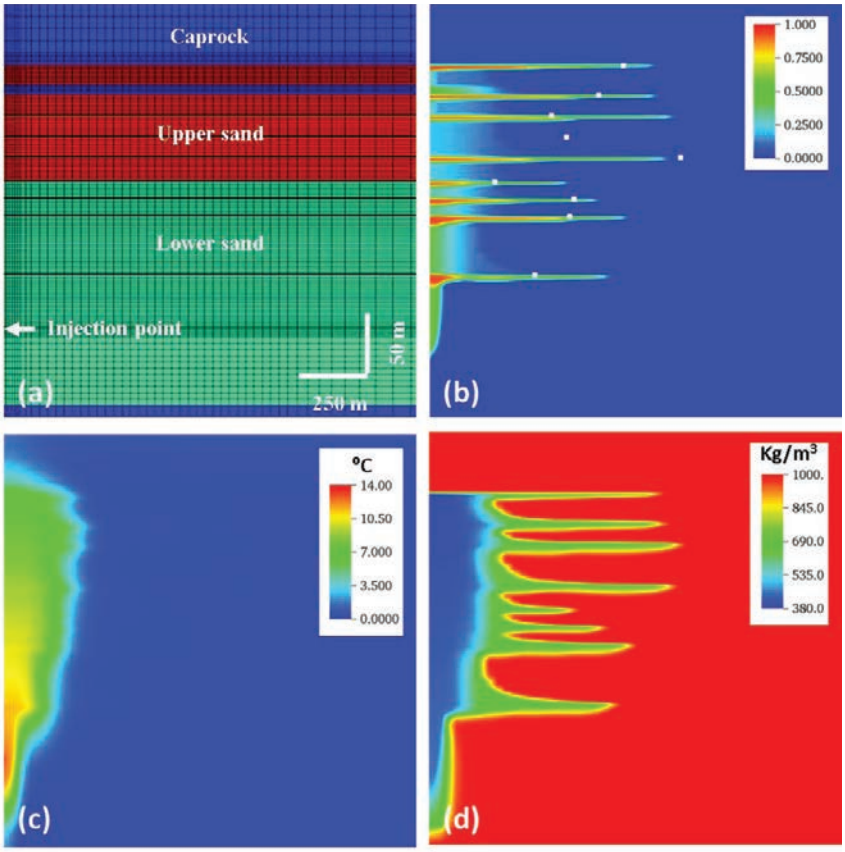

Fig. 7. 2D axisymmetric reservoir model showing the effect of injecting CO_2 at 48 ºC into a cooler reservoir. The reservoir temperature at the injection point (labelled) is ~35 ºC. (a) Simulation mesh, (b) CO_2 saturation in the reservoir, (c) thermal anomaly, and (d) CO_2 density. The simulation time-step corresponds to the 2006 seismic monitor survey. The radial equivalent extents of each seismically observed CO_2 layer in the plume are marked with a white square in (b).

The fluid temperature anomaly (Fig. 7c) shows an axial column of elevated fluid temperatures extending above the injection point to the top of the reservoir, undergoing Joule-Thomson cooling as the CO_2 expands. The thermal imprint of the rising column extends to a radius of around 350 m from the injection well. This is because of radial heat loss from the column into the surrounding reservoir and vertical heat loss into both the caprock and underlying reservoir. The thermal anomaly at the injection point is around +14 ºC, corresponding to the temperature difference between the injected CO_2 and the ambient reservoir. Above the injection point the temperature anomaly reduces to +7 ºC at the reservoir top and reduces further radially, such that it becomes negligible at distances more than about one third of the full layer spread.

Density distributions within the CO_2 plume (Fig. 7d) show a warm axial core with a density of 380-450 kg/m^3 which increases to around 730 kg/m^3 as the plume cools radially toward background reservoir temperatures. The mean CO_2 density in the top sand-wedge is around 685 kg/m^3, which agrees with an estimated density of 675 +/- 20 kg/m^3 based on gravity modelling [7]. The dynamic viscosity ranges from 40-60 μPa.S.

4. 3D reservoir simulation modeling

A 3D reservoir model of the top sand wedge was built using two simulators PFLOTRAN [11] and ECLIPSE 100 [12]. The simulation grid was constructed from depth-converted seismic travel-time picks of the top reservoir surface

and the top of the mudstone layer separating the top sand-wedge from the rest of the Utsira reservoir. The top reservoir surface was depth-converted using an overburden interval velocity function calculated from velocity surveys in nearby exploration wells. An interval velocity of 2050 m/s was used for the top sand-wedge itself.

A series of ECLIPSE 100 simulations were run to investigate the effect of permeability anisotropy on the distribution of CO_2 in the reservoir. ECLIPSE 100 implements a black oil model, in which fluid properties are interpolated as a function of pressure from a user-supplied lookup table. This makes for rapid run times, allowing for a high resolution grid and multiple realisations using different parameters. The ECLIPSE mesh had 60x111x24 cells in the X, Y and Z directions respectively, with horizontal cell dimensions of 50x50 m. The cell thickness varied from 6 m at the base of the model to 0.1 m at the top, to capture the detailed topography of the reservoir-caprock interface. The black oil parameters were calculated using a CO_2 density given by the Span and Wagner equation-of-state [13] and the methodology published by Hassanzadeh et al [14].

PFLOTRAN was used to investigate the effects of CO_2 temperature on the growth of the plume. This fully-coupled compositional simulator is computationally intensive, so a coarser vertical grid resolution of 2 m was used in these simulations, although the horizontal cell dimensions were again 50x50 m. The internal fluid property module supplied with PFLOTRAN was used to compute the density and viscosity of CO_2 as a function of temperature and pressure, again this used the Span and Wagner equation of state for pure CO_2 [13].

Both models were subject to broadly equivalent boundary conditions. The top and base of the reservoir were assumed to be impermeable, while the north, south, east and west boundaries were maintained at hydrostatic pressure. In the case of ECLIPSE 100, this was achieved using a large pore volume multiplier to simulate a connected open aquifer. The mass of CO_2 injected into the top sand-wedge was calculated from seismic observations, based on volumetric analysis assuming a flat CWC. The calculations are described by Chadwick & Noy [3] and their results are comparable to values published in the Sleipner benchmark model [1].

4.1. The effect of permeability heterogeneity and channeling

Permeability heterogeneity is a key factor controlling the flow of CO_2 in sand or sandstone reservoirs. High resolution seismic data acquired over Sleipner in 2010 [17] have shown that the top sand-wedge comprises a series of channels running from north to south across the survey area (Figs. 2, 5b). The flow properties of these channels have not been directly measured, but as discussed above, well logs (Fig. 4) and borehole pumping tests suggest that they might well comprise sand with significantly higher bulk permeability than the main Utsira Sand reservoir.

Three ECLIPSE 100 flow simulations were run to test the potential effects of permeability heterogeneity on the distribution of CO_2 in the reservoir. CO_2 saturation distributions for each model, displayed at selected simulation time-steps corresponding to 3D seismic monitor surveys, are compared with the CWC as measured on the seismic data (Fig. 8).

A uniform permeability of 8 Darcy was used in the first simulation (Fig. 8a), which represents our upper bound for the Utsira Sand consistent with the borehole pumping tests at Oseberg and Grane (see 2.1 above). This model gives a reasonable first-order match to the observed CWC, with the CO_2 rising to the top of the sand-wedge and spreading to infill caprock topography. The history-match improves generally with time, but the simulation cannot fully replicate the rapid north-directed spreading observed on seismic data.

The second simulation incorporated an anisotropic permeability distribution, 3 Darcy east-west and 8 Darcy north-south (Fig. 8b). This did not improve the history-match. Reduced permeability in the east-west direction slows the flow of CO_2 into the prominent north trending channel (blue arrow Fig. 5b), and the amount of north-directed spreading is actually reduced compared to the uniform permeability model.

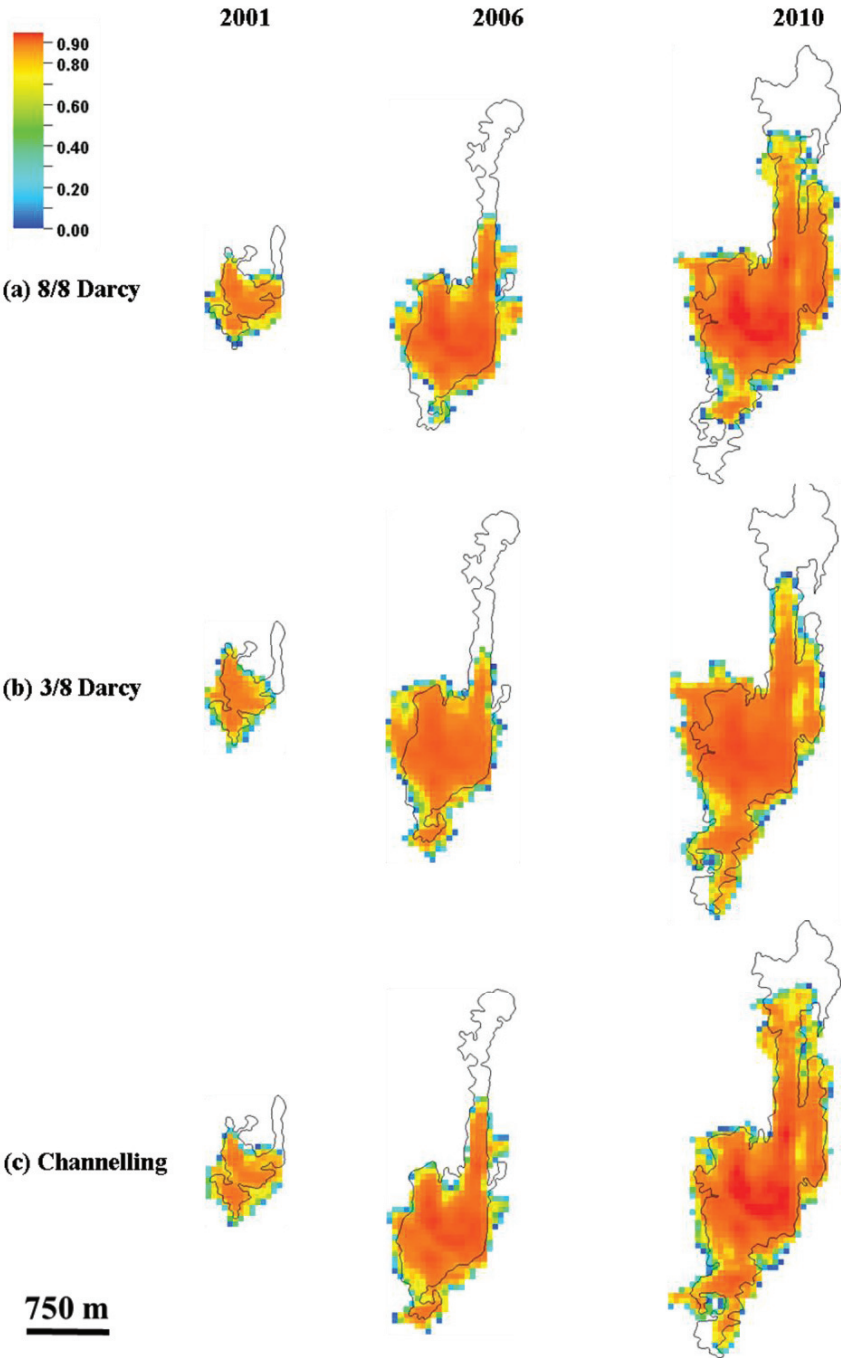

Fig. 8. Gas saturation distributions for the top CO_2 layer in the Sleipner plume at simulation time steps corresponding to selected 3D seismic monitor surveys. The CWC observed on the seismic data is shown as a black polygon. The simulations show the effects of permeability heterogeneity on the migration of CO_2 in the reservoir.

The best fit to the observed CO_2 distribution was obtained by the third simulation (Fig. 8c) which incorporated a connected high permeability channel within the top sand-wedge. The permeability field was computed from the isochore map (Fig. 5b), by assigning enhanced permeability to any area where the top sand-wedge thickness exceeded 20 ms (about 20 metres). Thus the channel contained within the red polygon in Fig. 5b was assigned a permeability of 8 Darcy, whereas outside the channel, permeability was set at 3 Darcy, as measured on the 15/9-A23 core samples. The resulting CO_2 saturation distribution (Fig. 8c) is not quite able to reproduce the observed CWC by 2010, but given the model simplicity, with no special tuning, it represents an excellent match to the seismic observations.

5. Thermal effects on flow properties

The preferred model, with heterogeneous permeability based on channel features, provides a good history-match to seismic measurements for the topmost layer of the Sleipner plume (compare Figs. 1 and 8c). However, the model does not quite fully replicate the observed spreading rate along the prominent north-south channel system (Fig. 5b) and it might be the case that some modification of fluid properties could further increase migration velocity.

The plume thermal structure (section 3) suggests that CO_2 will arrive in the top sand-wedge at a temperature of ~37 ºC, some 7 ºC warmer than the reservoir background (Fig. 7). The warm CO_2 will have a reduced density (~505 kg/m^3) and viscosity (c~36 μPa.s) compared with CO_2 that has cooled to the background temperature of ~30 ºC (725 kg/m^3 and 60 μPa.s respectively).

Using the preferred channel-based permeability distribution, a thermal conductivity of 3 W/m.K, and a specific heat capacity of 1000 J/(kg.K)[15, 16], temperature and CO_2 saturation distributions were modelled for CO_2 entering the top sand-wedge at ambient reservoir temperature (Fig. 9a, b) and for CO_2 entering at 37 ºC (Fig. 9c, d). The thermal anomaly spreads away from the injection point (Fig. 9c) for around 750 m, before decaying to just above the background reservoir temperature as heat is conducted into the surrounding rock mass. The resulting increase in CO_2 mobility is insufficient to induce anything but a very minor increase in north-directed spreading (Fig. 9b, d), although careful examination of the northern leading-edge of the CWC shows that warm CO_2 does spread slightly farther than CO_2 at reservoir temperature.

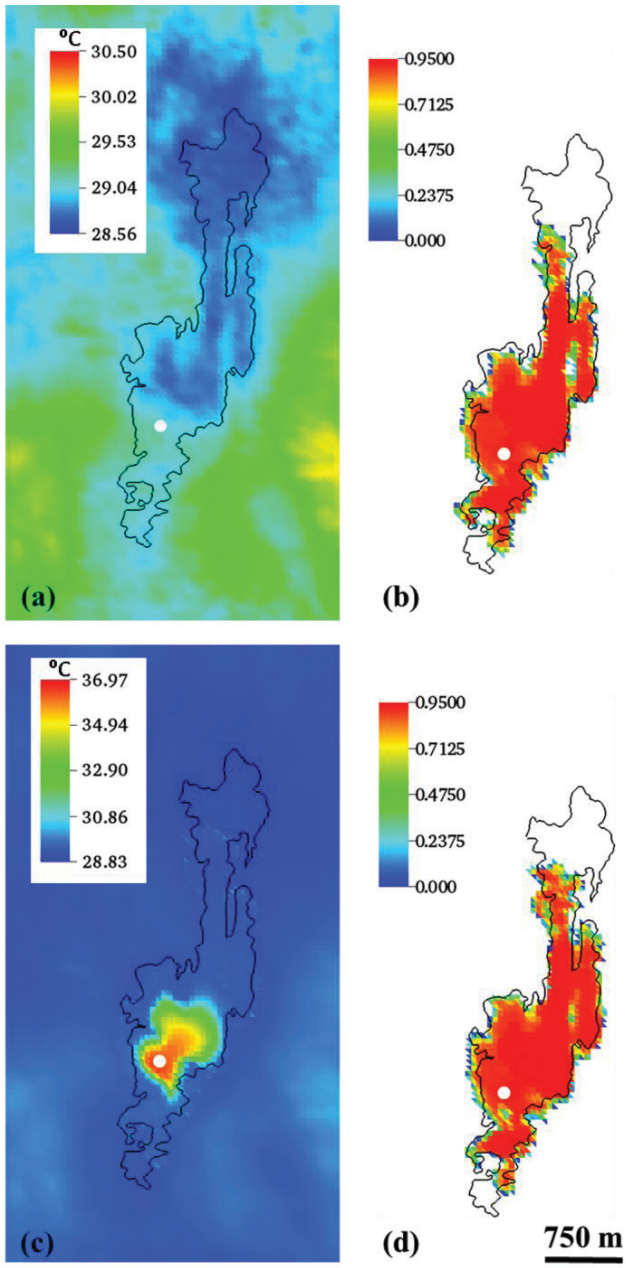

Fig. 9. The effect of injecting warm CO_2 into the top sand-wedge. (a) Background temperature distribution at the top of the reservoir. (b) CO_2 distribution at the time of the 2010 seismic monitor survey, assuming the CO_2 enters the top sand-wedge at the background reservoir temperature. (c) Thermal anomaly caused by CO_2 entering the top sand-wedge at a temperature of 37 ºC. (d) Resulting CO_2 distribution at the time of the 2010 seismic monitor survey. Black polygon denotes extent of the CWC measured on the 2010 seismic monitor survey. The location of the feeder chimney through which the CO_2 enters the sand-wedge from below is shown as a white circle.

6. Discussion

There have been a number of attempts to history match the growth of the topmost CO_2 layer in the Sleipner plume [1, 2, 3, 4, 5, 6]. Traditionally, the Darcy flow models have failed to fully replicate the observed distribution of CO_2 at Sleipner, leading a number of authors to invoke invasion-percolation (IP) theory to improve the match between seismic and simulator [5, 6]. IP simulators lack time-dependence, which severely limits their utility for future performance prediction. This is a significant disadvantage [18].

This contribution does not seek to compare the relative merits of different modelling techniques applied to carbon storage, but rather was carried out to investigate the effects of reservoir permeability heterogeneity and plume temperature on CO_2 migration at the reservoir top. In particular we re-examined the geological basis for setting the key reservoir flow parameters, developing a geological model constrained by integrating the seismic, borehole and laboratory data in a way that has not been previously achieved. By taking upper and lower permeability bounds of 3 and 8 Darcy, fully consistent with the integrated data analysis, it has proven possible to achieve a satisfactory first-order match to the distribution of CO_2 observed on seismic data (Fig. 8a). Introduction of a heterogeneous permeability field containing laterally constrained high permeability north-south channels gave a further improvement in the history-match (Fig. 8c).

Including thermal effects in the modelling did not significantly improve the history-match. On the other hand, we took no account of the likely presence in the CO_2 of around 2% methane. This will have the effect of increasing fluid mobility and would produce an even better match to the observed layer migration.

7. Conclusions

Detailed flow simulation history-matching of the topmost CO_2 layer at Sleipner has proven challenging. This study has focused on two key parameters affecting CO_2 migration mobility, namely reservoir permeability heterogeneity and fluid temperatures within the CO_2 plume. Re-examination of available geological information, integrating core, geophysical log and seismic datasets indicates that there is scope for a substantial revision of the basic premise for flow properties in the topmost reservoir sand.

Inclusion in the reservoir flow model of higher permeability channels, as observed on high resolution seismic data, is consistent with regional water production permeability data from the Utsira Sand, and markedly improves the fit between reservoir flow simulations and seismic observations of CO_2 layer spread. Modelling temperature distribution within the evolving plume suggest that CO_2 enters the top sand layer at a temperature of around 37 ºC, some 7 ºC warmer than the ambient reservoir. This reduces the density and viscosity of the CO_2 over distances up to around 350 m from the feeder-point. But whilst this increases CO_2 mobility in the central parts of the layer, it does not affect its more distal parts and so does not significantly further improve the fit between seismic and simulation.

The remarkable monitoring dataset acquired as part of the Sleipner CO_2 injection operation has provided a unique opportunity to history-match a growing CO_2 plume. The results presented here suggest that CO_2 flow in the spreading topmost layer of the plume can be satisfactorily modelled using a Darcy flow simulator, provided that reservoir flow parameters are carefully constrained to be consistent with all of the available information, including core, geophysical log and seismic data.

Acknowledgements

The work was carried out under the DiSECCS project, funded by the UK Engineering and Physical Sciences Research Council, and is published with permission of the Executive Director, British Geological Survey (NERC). Additional support has come from the BIGCCS Centre, performed under the Norwegian research program Centres for Environment-friendly Energy Research (FME). The authors acknowledge the following partners for their contributions: ConocoPhillips, Gassco, Shell, Statoil, TOTAL, GDF SUEZ, and the Research Council of Norway (193816/S60). Statoil Petroleum AS, LOTOS Exploration and Production Norge AS, ExxonMobil Exploration & Production Norway AS, and Total E&P Norge AS are thanked for provision of the seismic data.

References

[1] Singh, V. P., Cavanagh, A., Hansen, H., Nazarian, B., Iding, M., Ringrose, P. S. Reservoir modeling of CO_2 plume behavior calibrated against monitoring data from Sleipner, Norway. *SPE-134891-MS* 2010; 1-18.

[2] Chadwick, R. A., Noy, D. J. Underground CO_2 storage: demonstrating regulatory conformance by convergence of history-matched modeled and observed CO_2 plume behavior using Sleipner time-lapse seismics. *Greenhouse Gas Sci Technol* 2015; **5**:305–322.

[3] Chadwick, R. A., Noy, D. J. History-matching flow simulations and time-lapse seismic data from the Sleipner CO_2 plume. *Geological Society, London, Petroleum Geology Conference Series* 2010; **7**:1171–1182.

[4] Zhu, C., Zhang, G., Lu, P., Meng, L., Ji, X. Benchmark modeling of the Sleipner CO_2 plume: calibration to seismic data for the uppermost layer and model sensitivity analysis. *International Journal of Greenhouse Gas Control* 2015; **43**:233-246.

[5] Cavanagh, A. Benchmark Calibration and Prediction of the Sleipner CO_2 Plume from 2006 to 2012. *Energy Procedia* 2013; **37**: 3529–3545.

[6] Cavanagh, A. J., Haszeldine, R. S. The Sleipner storage site: capillary flow modeling of a layered CO_2 plume requires fractured shale barriers within the Utsira Formation. *International Journal of Greenhouse Gas Control* 2014; **21**: 101–112.

[7] Alnes, H., Eiken, O., Nooner, S., Sasagawa, G., Stenvold, T., Zumberge, M. Results from Sleipner gravity monitoring: updated density and temperature distribution of the CO_2 plume. *Energy Procedia* 2011; **4**: 5504–5511.

[8] Chadwick, R.A., Kirby, G.A., Holloway, S., Gregersen, U., Johannessen, P.N., Zweigel, P., Arts, R. Saline Aquifer CO_2 Storage: geological characterisation of the Utsira Sand reservoir and caprocks. *British Geological Survey Commissioned Report* 2002; **CR/02/153C**: 1-18.

[9] Lindeberg, E., van der Meer, B., Moen, A., Wessel-Berg, D., Ghaderi, A. Saline Aquifer CO_2 Storage (SACS): Fluid and core properties and reservoir simulation. *SINTEF Petroleum Research Technical Report* 2000; **54.5148.00/02/00**: 1-42

[10] Eidven, T., Riis, F., Rasmussen, E.S., Rundberg, Y. Investigation of Oligocene to Lower Pliocene deposits in the Nordic offshore area and onshore Denmark. *NPD Bulletin* 2013; **10**: 1-46

[11] Lichtner, P. C., Hammond, G. E., Lu, C., Karra, S., Bisht, G., Andre, B., et al. *PFLOTRAN User Manual*. 2015.

[12] Schlumberger. *Eclipse Technical Description 2011.1*. 2011.

[13] Span, R., Wagner, W. A new equation of state for carbon dioxide covering the fluid region from the triple-point temperature to 1100 K at pressures up to 800 MPa. *Journal of Physical and Chemical Reference Data*. 1996; **25**:1509–1596.

[14] Hassanzadeh, H., Pooladi-Darvish, M., Elsharkawy, A. M., Keith, D. W., Leonenko, Y. Predicting PVT data for CO_2-brine mixtures for black-oil simulation of CO_2 geological storage. *International Journal of Greenhouse Gas Control* 2008; **2**: 65–77.

[15] DeMarsily, G. *Quantitative Hydrogeology*, Academic Press; 1986

[16] Engineering Toolbox. Thermal conductivities of some common materials and gases. *www.EngineeringToolbox.com* 2016.

[17] Furre, A. K., Eiken, O. Dual sensor streamer technology used in Sleipner CO_2 injection monitoring. *Geophysical Prospecting* 2014; **62**: 1075–1088.

[18] Oldenburg, C. M., Mukhopadhyay, S., Cihan, A. On the use of Darcy's law and invasion-percolation approaches for modeling large-scale geologic carbon sequestration. *Greenhouse Gases: Science and Technology* 2016; **6**: 19–33.